Article

Enhancing Environmental Protection in Oil and Gas Wells through Improved Prediction Method of Cement Slurry Temperature

Bo Feng [1], **Jin Li** [1], **Zaoyuan Li** [1,*], **Xuning Wu** [1,2,*], **Jian Liu** [1], **Sheng Huang** [1] and **Jinfei Sun** [3]

[1] Petroleum Engineering School, Southwest Petroleum University, Chengdu 610500, China; fengboswpu@126.com (B.F.)
[2] Research Centre of Energy Storage Technologies, Clausthal University of Technology, 38640 Goslar, Germany
[3] School of Sciences, Southwest Petroleum University, Chengdu 610500, China
[*] Correspondence: swpilzy@swpu.edu.cn (Z.L.); 201911000102@stu.swpu.edu.cn (X.W.)

Abstract: Accurate cement slurry temperature prediction is a prerequisite for improving cementing quality and ensuring wellbore integrity and sealing of oil and gas wells. It plays a crucial role in preventing "gas migration" and "sustained casing pressure" problems and reducing environmental pollution. The construction links before the start of cementing are neglected by the existing prediction methods, and thus, it is not reasonable to assume initial temperature conditions. In this paper, a two-dimensional transient temperature field model for cementing is developed and its reasonableness is verified. The distribution of wellbore and formation temperature fields at cementing beginning is calculated. In addition, the influence rules of several factors on the cement slurry circulation temperature are calculated and discussed. The results show that the initial temperature varies significantly and that each factor affects the fluid circulation temperature in different ways and to different degrees. If the circulating wash operation before cementing is considered, the temperature field decreases in the downhole section and increases in the uphole section compared to the assumption that the initial condition is the original formation temperature. By correcting the initial conditions, the accuracy of cement slurry circulation temperature prediction can be improved.

Keywords: cement slurry temperature; initial condition; transient temperature field models; circulation temperature distribution; influence factors

1. Introduction

Cementing operations are directly related to the integrity between the casing and the formation and to achieving effective sealing of oil and gas in the formation [1]. It is essential to minimize the setting time of the cement slurry in order to achieve an effective seal on the formation fluids. The cement slurry sets as soon as it returns to the annulus [2]. Controlling the setting time of cement slurry depends on the construction process and the cement slurry's properties. Temperature is one of the most critical parameters for cement construction design and cement slurry formulation design [3]. Prediction of cement slurry bottom circulation temperature (BHCT) is often conservative. For example, the most commonly used American Petroleum Institute (API) calculation method generally overestimates the BHCT value [4,5]. Over-prediction of temperature generally leads to over-dosing of retarders in cement slurry formulation design, which results in long cement slurry setting times [6,7].

The long setting time of the cementing slurry causes fluids in the formation to enter the wellbore. This may create flow paths in the annular space between the casing string and the borehole walls. In petroleum terminology, this phenomenon is referred to as "flow behind cement", "gas migration", "annular migration", or, more recently, "sustained casing pressure (SCF)" [8–10]. After this phenomenon occurs in gas wells, the wellhead pressure continues to rise as the gas continues to move up and accumulate at the top of

the wellbore [11–14]. If the fluids from the formation contain CO_2, H_2S, etc., it can corrode the cementite and casing, which may lead to a wellhead leak in severe cases. This can have a serious impact and safety risk for oil and gas well production. The migration of petroleum hydrocarbons, injected brines, or other toxic waste fluids may cause pollution of the atmosphere, surface waters, or groundwater aquifers [8]. Inaccurate cement slurry temperature prediction can make the cement slurry take a long time to set, which in turn can lead to production safety and environmental pollution problems in oil and gas wells.

The numerical solution of the temperature field is generally considered to be the most reliable method for predicting the temperature of cement slurry [15,16]. The reason for this is that it incorporates a broader range of influencing factors and is more consistent with changes in wellbore and formation temperature fields. Inevitably, the initial conditions of a numerical calculation have an impact on the final outcome. Due to operational processes such as drilling, through-hole, electrical logging, lowering into casing, and circulating drilling fluid before cementing, the temperature field of the wellbore and formation before cementing has changed and is no longer the original temperature of the formation. It is necessary to establish a reasonable initial temperature condition for calculating the cementing slurry temperature.

In the current method of calculating cementing slurry temperature, the actual temperature conditions of the wellbore and formation are almost always overlooked. The commonly used initial temperature conditions are similar to those used for drilling fluid circulation temperature calculations during drilling [6,17]. This assumes that the temperature field is the original formation temperature distribution. Sump (1973) [18] developed a numerical calculation program based on Raymond's temperature field model (1969) [19]. The program can be used to calculate the circulation temperature of cement slurry. The model is constructed based on the temperature field during the drilling process and assumes that the initial temperature distribution is the original formation temperature, which is reasonable for calculating the drilling fluid circulation temperature, but it is obviously not reasonable to be used for calculating the cement slurry circulation temperature. Ran (2019) [20] conducted a computational fluid dynamics (CFD) simulation study with finite element software to analyze cement slurry circulation temperature characteristics for offshore cementing operations. The actual temperature field distribution before cement injection was also neglected. Rui (2021) [16] assumes that the drilling fluid in the wellbore rests for a period of time before cement injection and the temperature field returns to the original formation temperature. In this manner, a CFD simulation study of cement slurry circulation temperature is conducted. The cement injection operation is preceded by a cementing circulation wash, during which drilling fluid is continuously circulated in the wellbore. The wellbore and formation temperature distribution at the end of the drilling fluid circulation is clearly not the original formation temperature. Consequently, to obtain the initial temperature conditions for cementing, the temperature field distribution at the end of the circulation wash must be determined.

The circulation wash is performed before cementing and after the casing has been lowered. After a production well is drilled, the well will be through-hole, logged, and cased. During this period, the drilling fluid in the wellbore is mostly at rest. After a few days of heat exchange, the temperature of the fluid, casing, and formation around the borehole will slowly resume to the original formation temperature [21–24]. Therefore, it is more reasonable to assume that the temperature field at the end of the lowering casing operation is the original formation temperature than to assume at the start of cement injection. There will be a significant reduction in calculation errors caused by the initial temperature conditions. In this paper, a two-dimensional transient temperature field model for cementing wells is constructed to calculate and analyze the changes in wellbore and formation temperatures during the cementing circulation wash. It is also used to obtain the temperature field distribution at the end of circulation. For subsequent cement slurry circulation temperature calculations, this temperature field provides more reasonable initial temperature conditions. In addition, using the developed temperature field prediction

model, eight factors affecting the fluid circulation temperature in the wellbore are calculated and discussed, and the degree of influence is ranked.

2. Methods

2.1. Physical Model

Drilling fluid is pumped into the casing and flows down the casing at the beginning of the cementing cycle wash. The drilling fluid flows and transfers heat in the axial direction, and convective heat exchange occurs with the casing wall in the radial direction. Upon reaching the bottom of the well, the drilling fluid in the casing and the drilling fluid in the annular space mix together. The drilling fluid continues to flow upward along the annular space, and the drilling fluid flows and transfers heat in the axial direction, and convection heat exchange occurs with the formation and the outer wall of the casing in the radial direction, respectively.

The entire temperature field system can be divided into four regions as shown in Figure 1. The first region is the fluid in the casing, with temperature T_c; The second region is the casing string, temperature T_w; The third region is the annular fluid, temperature T_a; The fourth region is the formation, temperature T_f.
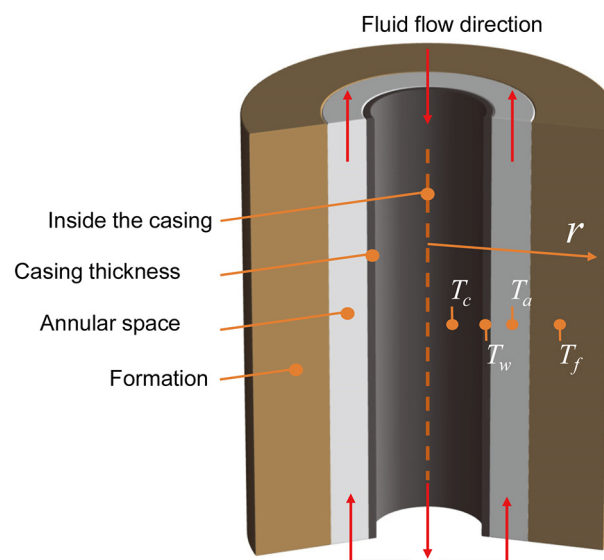

Figure 1. Schematic representation of wellbore and formation temperature fields.

2.2. Assumptions of the Model

To construct the energy balance equations, the following assumptions are made based on the characteristics of the heat exchange between the wellbore and the formation [19,25,26]:

(1) The study considers only the energy equation and ignores the momentum and mass equations;

(2) The thermal properties (specific heat capacity, thermal conductivity) of the fluid and formation rocks are isotropic, without regard to circumferential differences, and the thermal physical properties are averaged and do not change with temperature or pressure;

(3) The wellbore and formation are axisymmetric along the centerline of the wellbore and flow along the inside of the tube and in the annulus, disregarding the flow boundary layer and temperature boundary layer and disregarding the temperature gradient in the radial direction;

(4) The influence of axial heat transfer in the fluid circulation process is small, ignoring axial heat transfer; frictional heat generation (viscous dissipation energy) in the flow process is involved in the temperature calculation as a heat source term;

(5) Heat exchange in the formation is mainly heat conduction, and fluid flow and convective heat transfer are not considered.

(6)   The temperature field distribution in the bare borehole is studied. The complex structure formed by the cemented well is neglected in the upper part of the wellbore, which includes cement stone, multilayer casing, drilling fluid, and antecedent fluid.

2.3. Governing Equations

According to the assumptions, the physical structure can be simplified to a two-dimensional axisymmetric geometry, as shown in Figure 2. The formation region is treated with a two-dimensional grid and the rest of the regions are gridded axially in one dimension. The energy balance equations of the four regions are constructed separately [19,26,27].

(1)   Energy balance equation inside the casing

$$Q_c + \rho_1 q C_1 \frac{\partial T_c}{\partial z} + 2\pi r_{ci} h_{ci}(T_w - T_c) = \rho_1 C_1 \pi r_{ci}^2 \frac{\partial T_c}{\partial t} \tag{1}$$

where r is the radial distance from the symmetry axis and the axial direction; z is the axial coordinate; Q_c is the heat generated by the frictional pressure drop of the drilling fluid per unit length in the casing; ρ_1 is the drilling fluid density inside the casing; q is the drilling fluid circulation displacement; C_1 is the drilling fluid constant volume specific heat capacity; r_{ci} is the inner radius of the casing; h_{ci} is the convective heat transfer coefficient between the drilling fluid inside the casing and the inner wall of the casing.
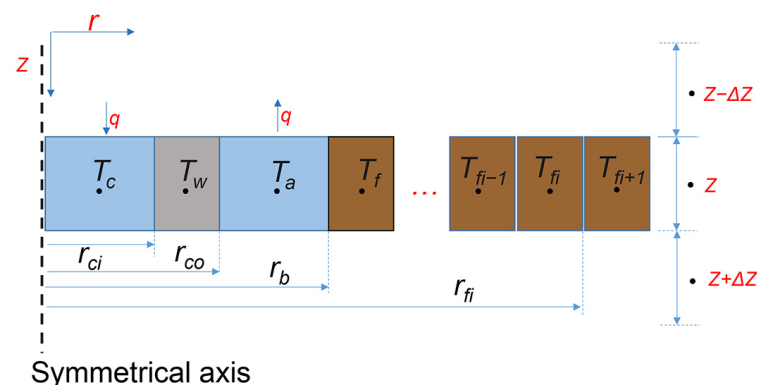

Figure 2. Two-dimensional axisymmetric schematic of wellbore and formation (left region ignored).

The temperature of the fluid inside the casing is determined by the heat transfer and frictional heat generation of the fluid flow in the axial direction and convective heat transfer with the casing in the radial direction. In Equation (1), the second term on the left represents heat transfer from the axial flow of the fluid. The third term on the left represents the convective heat transfer between the fluid in the radial direction and the inner wall of the casing. The right side represents the fluid's heat accumulation as a function of time.

(2)   Energy balance equation of the casing

$$\lambda_2 \frac{\partial^2 T_w}{\partial z^2} + \frac{2 r_{co} h_{co}}{r_{co}^2 - r_{ci}^2}(T_a - T_w) + \frac{2 r_{ci} h_{ci}}{r_{co}^2 - r_{ci}^2}(T_c - T_w) = \rho_2 C_2 \frac{\partial T_w}{\partial t} \tag{2}$$

where λ_2 is the thermal conductivity of the casing steel; r_{co} is the radius of the outer diameter of the casing; h_{co} is the convective heat transfer coefficient between the annular drilling fluid and the casing; ρ_2 is the density of the casing steel; C_2 is the specific heat capacity of the casing steel.

The temperature of the casing itself is determined by convective heat transfer and axial heat conduction of the fluid inside and outside the casing. In Equation (2), the first term on the left side represents the axial heat transfer. The second and third terms on the left side represent convective heat transfer outside the casing and convective heat transfer inside the casing, respectively. The right side represents the casing's heat accumulation as a function of time.

(3)   Energy balance equation of annular fluid

$$\rho_1 q C_1 \frac{\partial T_a}{\partial z} + 2\pi r_b h_b \left(T_f - T_a \right) + 2\pi r_{co} h_{co} (T_w - T_a) + Q_a = \rho_1 C_1 \pi \left(r_b^2 - r_{co}^2 \right) \frac{\partial T_a}{\partial t} \quad (3)$$

where r_b is the borehole radius; h_b is the convective heat transfer coefficient between the well wall and the annulus fluid; Q_a is the heat generated by the frictional pressure drop per unit length of the annulus drilling fluid.

The temperature of the annulus fluid is determined by the heat transfer and frictional heat energy of the fluid flow in the axial direction and convective heat transfer with the well wall and casing in the radial direction. In Equation (3), the first term on the left side represents the fluid flow heat transfer. The second and third terms represent convective heat transfer between the fluid and the well wall and casing, respectively. The right side represents the fluid's heat accumulation as a function of time.

(4)   Energy balance equation of the formation

$$\frac{\lambda}{r} \frac{\partial}{\partial r} \left(r \frac{\partial T_f}{\partial r} \right) + \lambda_3 \frac{\partial^2 T_f}{\partial z^2} = \rho_3 C_3 \frac{\partial T_f}{\partial t} \quad (4)$$

where λ_3 represents the thermal conductivity of the stratum; ρ_3 represents the density of the stratum; and C_3 represents the specific heat capacity of the stratum.

The formation's temperature is determined by its own axial and radial heat transfer. In Equation (4), the left two terms represent radial heat transfer and axial heat transfer, in that order. The right side represents the formation 's heat accumulation as a function of time.

2.4. Initial and Boundary Conditions

To solve the equations system formed by Equations (1)–(4), it is necessary to set initial and boundary conditions.

The temperature field distribution at the end of the lowering casing operation (before the start of the circulation wash) is the same as the original formation temperature.

$$T_c(z, t = 0) = T_a(z, t = 0) = T_f(z, t = 0) = T_s + Gz \quad (5)$$

where T_s is the temperature of the ground surface and G is the ground temperature gradient.

The temperature of the injected drilling fluid can be measured.

$$T_c(z = 0) = T_{in} \quad (6)$$

The drilling fluid is at the same temperature at the well bottom.

$$T_c(z = H) = T_a(z = H) \quad (7)$$

The original formation temperature is always maintained if the formation is beyond the range of fluid influence, as in Equation (8), where r_{ei} is the distance of fluid influence on the formation radially

$$T_f(r \to r_{ei}, z, t) = T_s + Gz \quad (8)$$

The axis of centrosymmetry, the formation at the bottom of the well, and the top and bottom of the casing string are assumed to be adiabatic boundaries.

2.5. Numerical Solution

The finite difference method is applied to discretize the established wellbore temperature model in space and time for the entire geometric structure, as shown in Figure 2, and in time in an implicit form. The partial differential equation is made to be transformed into an algebraic equation. The fluid inside the casing, the casing string, and the annulus fluid were meshed in one dimension along the axial direction, and 100 cells of the same size are formed, respectively. Three grid cells of unequal size are formed due to neglecting

the temperature gradient in the radial direction of the fluid, casing column, respectively, which is the third assumption condition of the model. The formation is gridded in two dimensions in the radial and axial directions, respectively, and 100 cells of the same length are formed in the axial direction as well. For better analysis of the radial temperature variation, the grid cells are not uniformly sized, and the closer to the borehole wall, the smaller the size. The specific discretization process of the equation and the form of the discretized equation are similar to Marshall (1982) [27] and Yang (2015) [28], and the section is omitted in this paper.

The equation for the convective heat transfer coefficient is derived from Petukhov (1970) [29].

$$h = \frac{Nu\lambda}{D} \tag{9}$$

$$Nu = \frac{(f/8)\mathrm{RePr}}{1.07 + 12.7(f/8)^{1/2}(\mathrm{Pr}^{2/3} - 1)} \tag{10}$$

$$f = (1.82 \ln \mathrm{Re} - 1.64)^{-2} \tag{11}$$

where h is the convective heat transfer coefficient; Nu, Re, and Pr are the Nusselt number, Reynolds number, and Prandtl number, respectively; and f is the friction coefficient.

3. Results and Discussion

Firstly, the reasonableness of the model is verified by comparing previous models. Then, the temperature field distribution at the end of the cementing circulation wash is calculated, and finally, the effects of various factors on the circulation temperature of the fluid are analyzed. The temperature field distribution at the end of the cementing circulation wash is the initial condition for calculating the cement slurry circulation temperature.

The calculation examples in this paper are derived from the Holmes (1970) [27,30] article and include circulating displacement volume, thermal physical properties, rheological parameters, etc., as shown in Tables 1 and 2. The example has been widely cited.

Table 1. Basic parameters for circulating temperature calculations.

Parameter	Value	Unit
Well depth	4572	m
Casing I.D.	0.15152	m
Casing O.D.	0.16828	m
Borehole size	0.21273	m
Ground temperature gradient	2.31	°C/100 m
Inlet temperature	23.89	°C
Surface temperature	15.28	°C
Drilling fluid n-value	0.71	-
Drilling fluid k-value	0.59	Pa·S^n
Circulating displacement volume	47.69	m^3/h

Table 2. Parameters of basic thermal physical properties.

	Drilling Fluid	Casing	Formation
Density (g/cm^3)	1.2	7.8	2.64
Specific heat capacity (J/(g·°C))	1.6747	0.4	0.83736
Thermal conductivity (W/(m·°C))	1.7307	43.75	2.2499

3.1. Verifying the Reasonability of the Models

The temperature field solution results are compared with the models of Hasan (1996) [31] and Yang (2015) [28]. The two models represent the steady state analytical model calculation method and the transient model numerical solution method, respectively. The former is

based on the Holmes model and the formation temperature analytical model is extended, which is widely accepted and often used as a control model for wellbore temperature field studies [17,32,33]. The latter builds on the Marshall model by considering the preceding cementing operation, where a composite structure of casing, cementing stone, or drilling fluid is formed.

A comparison of the temperature solution results for the three different models of wellbore annulus drilling fluid is shown in Figure 3. The three models have similar temperature profiles, with maximum bottom hole temperatures ranging from 94.5 to 98.1 °C, and the differences in the solution results are relatively small.
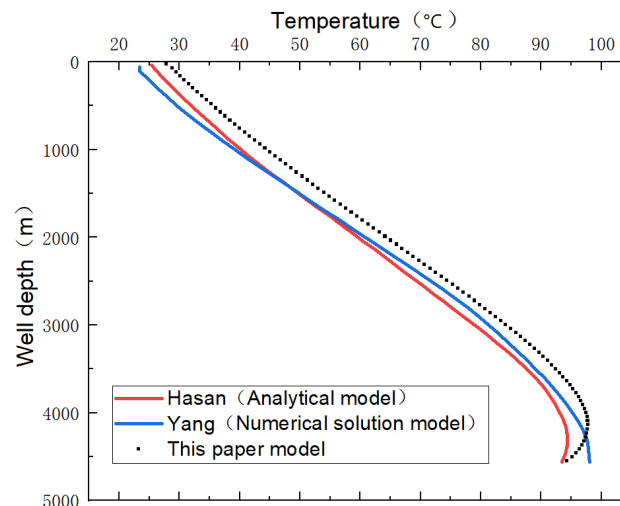
Figure 3. Comparison of temperature distribution (10 h circulation) of drilling fluids in the wellbore annulus for different models. The red curve in the graph represents Hasan's model [31], the blue curve represents Yang's model [28], and the black scatter plot represents the model in this paper.

The temperature profile of the annular drilling fluid solved by this model is closer to the shape of Hasan's analytical model, but the overall temperature is higher. Hasan's analytical model ignores the effect of the heat source term, frictional heat generation, on the temperature, and the temperature values will be low. The model also assumes a pseudo-steady state in the wellbore, where the fluid circulation time has a small effect on temperature. The wellbore in this paper is transient, and as the fluid flow time increases, the temperature at the bottom of the well in the model presented in this paper decreases further. There are moments of temperature equality between the results of these two model solutions.

The composite structure formed by the previous cementing operations is considered in Yang's model, which considers a higher heat flow between the formation and the annular fluid in the upper well section. This results in lower annular fluid temperatures near the wellhead than the model used in this paper. The model is used to calculate the circulation temperature during drilling. It takes into account the heat generated by the hydraulic pressure drop of the drill bit, resulting in a higher temperature at the bottom of the well.

The model solution results in this paper are in good agreement with other researchers' calculation results. There are some differences in the solution results due to differences in the construction of mathematical models, boundary conditions, convective heat transfer coefficient considerations, and numerical solution methods. However, it can be concluded that the results of the model solution are reasonable.

3.2. Calculating the Temperature Field Distributions for Cementing Circulation Wash

The drilling fluid temperature distribution is calculated at the end of the cementing circulation wash. A transient temperature model is constructed in this paper, and thus, the temperature distribution is different for different circulation times, as shown in Figure 4.
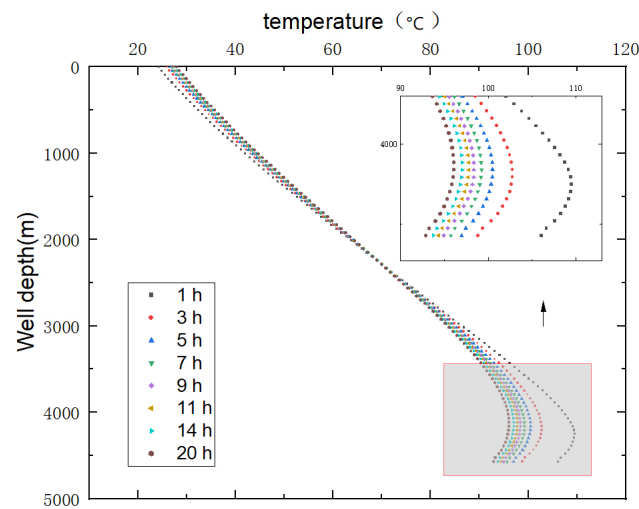
Figure 4. Distribution of drilling fluid temperature at different circulation times in the annulus.

As the circulation wash time increases, the well bottom temperature gradually decreases in the annulus. The decrease is very rapid at the beginning and gradually slows down after the circulation time reaches 9 h. The temperature distribution changes less and can be seen as starting to reach a pseudo-steady state. The calculations found that the wellbore volume is 143.25 m^3, and at a circulation flow rate of 47.69 m^3/h, the time to circulate three times is 9 h. The author's field research statistics found that cementing circulation wash operation is required to be cycled more than three times to ensure a uniform mix of drilling fluid in the wellbore and mud tank. Therefore, this paper only needs to calculate the temperature field distribution at three cycles (9 h).

The wellbore temperature field when the cementing circulation washed the well for 9 h, as shown in Figure 5. In the radial direction the drilling fluid in the casing, the casing string and the annular drilling fluid form a forward temperature difference, transferring heat in the reverse direction by convective heat exchange. Wellbore temperature field distribution: the fluid temperature in the casing is 15.28 to 94.41 °C, with the highest temperature at the bottom of the well; the casing string temperature is 26.58 to 97.1 °C; the fluid temperature in the annulus is 27.21 to 98.39 °C, with the highest temperature near 4160 m, the depth of the hot spot. The drilling fluid circulation temperature is 98.39 °C.
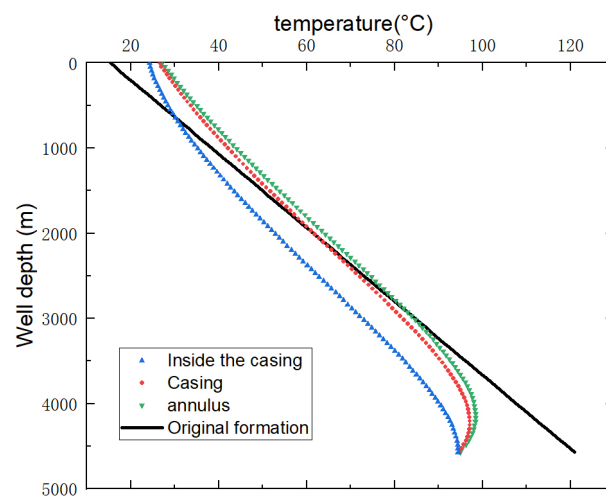

Figure 5. Wellbore temperature distribution (9 h circulation).

Distribution of temperature in the formation after 9 h of drilling fluid circulation, as shown in Figure 6. The temperature of the annular drilling fluid is close to the original temperature of the formation around 3000 m deep in the well, which can be defined as

"temperature stability depth". Drilling fluid in the annulus is heated by the formation below 3000 m and the formation is heated by drilling fluid in the annulus above 3000. The formation temperature at the bottom of the well is affected by drilling fluids by approximately 0.7 m. This is similar to previous studies' understanding [34,35].
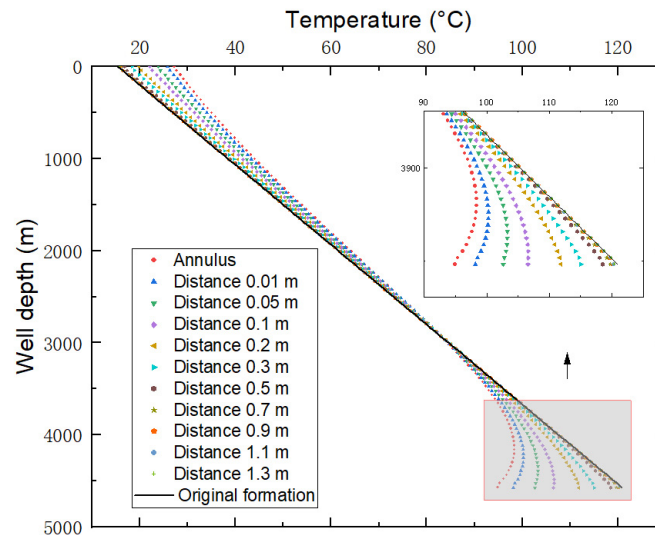

Figure 6. The temperature of the formation profile at different distances from the annulus (radial).

The temperature field consists of the wellbore temperature distribution (Figure 5) and the formation temperature distribution (Figure 6) at the end of the recirculation wash, which is the initial temperature condition for the next cementing operation. This is a more reasonable condition for the start of the cementing slurry circulation temperature calculation.

3.3. Analysis of the Factors Influencing Fluid Circulation Temperature

Based on the characteristics of cementing operations and the results of the survey, eight common influencing factors that are necessary to be discussed in this paper are presented, including circulation time, circulation flow, injected fluid temperature, ground temperature gradient, formation thermal conductivity, drilling fluid density, drilling fluid thermal conductivity, and drilling fluid specific heat capacity [27,36]. Assuming that other parameters remain constant, the influence rules of each individual factor are discussed and ranked based on their degree of influence on fluid circulation temperature.

3.3.1. Circulation Time

The change in drilling fluid temperature at different circulation times is analyzed using a controlled variable approach. The other parameters involved in the calculation remain unchanged.

According to Figure 4, the length of circulation time has a significant impact on the temperature of drilling fluid: the longer the circulation time, the lower the bottom hole temperature and the higher the outlet temperature; The wellbore temperature tends to stabilize, and the temperature distribution does not change much when the circulation time is greater than 9 h; The hot spot moves upward in depth with the extension of the circulation time.

3.3.2. Circulation Flow

In the annulus of this well, assume a circulation flow rate of 10–30 L/s, corresponding to a return velocity of 0.75–2.26 m/s. Other calculation conditions are assumed to be constant, including drilling fluid rheological parameters. When circulating for nine hours, the changes in wellbore temperature distributions at different flow rates are calculated and analyzed separately.

Some insights can be gained from Figure 7 and the corresponding data. From the full well axis upwards, as the flow rate increases at a well depth of approximately 2100 m, the effect is less; the annular temperature increases at 2100 m to the wellhead section; and the annular temperature decreases at 2100 m to the bottom of the well section with a large change in the bottom of the well temperature values. With increasing flow rate, temperature changes in the well bottom and wellhead sections gradually decrease. As the flow rate increases from 10 L/s to 15 L/s, the temperature of the bottom hole hot spot decreases by 8.1 °C and the outlet temperature increases by 2.7 °C. As the flow rate increases from 25 L/s to 30 L/s, the temperature of the hot spot at the bottom of the well decreases by 5.4 °C and the outlet temperature increases by 1.9 °C. The position of the hot spot continues to move upwards as the circulation flow rate increased. With a flow rate of 10 L/s, the well depth is 4251 m, and with a flow rate of 30 L/s, the position is raised by 574 m. As the flow rate increases, the difference between the hot spot temperature and the outlet temperature decreases from 78 °C to 41.7 °C.
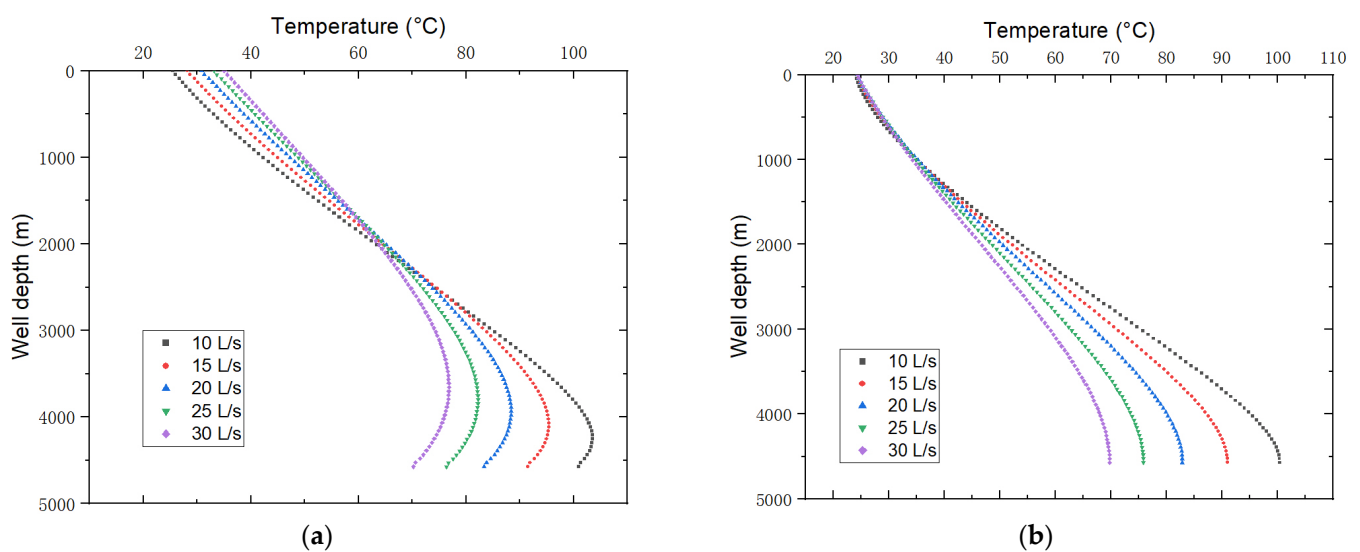

Figure 7. Drilling fluid temperature distribution for different circulation flows: (**a**) Drilling fluid temperature distribution in the annulus (**b**); Drilling fluid temperature distribution in the casing.

The reasons for the changes in the temperature distribution are analyzed. When the circulation flow rate is low, the drilling fluid is circulated for a longer period of time: over a week. More heat is gained by the drilling fluid from the formation in the lower section of the well, and more heat is lost by the cooling of the upper formation. This results in higher temperatures at the bottom of the well and lower temperatures returning to the wellhead, which is reversed when the flow rate is increased.

3.3.3. Injected Fluid Temperature

The temperature of the injected drilling fluid into the wellbore is influenced by a variety of factors, including seasonal temperature variations, differences in mud tank insulation, mud tank volume size, length of standing time, and differences in the thermophysical properties of the drilling fluid. To discuss the effect of drilling fluid injection temperature on the temperature distribution, an inlet temperature of 9 to 27 °C is assumed.

Some insights can be gained from Figure 8 and the corresponding data. As the temperature of the injection drilling fluid increases, the temperature of the entire well will also increase to varying degrees. As the depth of the well increases, the temperature increase value gradually decreases. When the inlet temperature increases by 3 °C and the outlet temperature increases by 1.6 °C, the temperature increases by 1.3 °C at 1000 m well depth, by 0.6 °C at 2000 m, and by 0.1 °C at the bottom of the well.
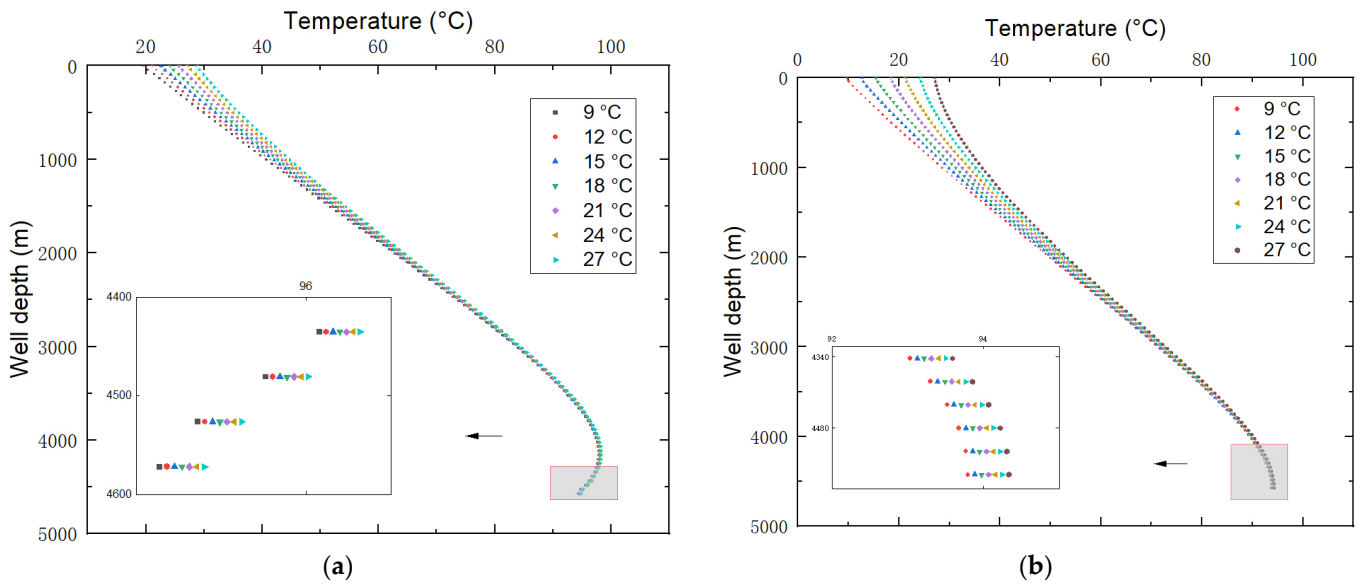
Figure 8. Distribution of drilling fluid temperature in the wellbore for different injection temperatures: (**a**) Drilling fluid temperature distribution in the annulus (**b**); Drilling fluid temperature distribution in the casing.

3.3.4. Ground Temperature Gradient

The ground temperature gradient directly responds to the rate of change of formation temperature with vertical well depth. Assuming a ground temperature gradient of 2.1–3.1 °C/100 m, the effect of different ground temperature gradients on the temperature distribution (9 h circulation) of drilling fluid is calculated and discussed.

As shown in Figure 9, some insights can be gained. The temperature of the drilling fluid circulation increases as the ground temperature gradient increases. For every 0.2 °C/100 m increase in the ground temperature gradient, the bottom hole temperature increases by about 6.7 °C in the casing and increases linearly. For every 0.2 °C/100 m increase in the ground temperature gradient, the hot spot temperature increases by about 7.12 °C in the annulus, and the temperature increase at the outlet is 0.63 °C and linear.
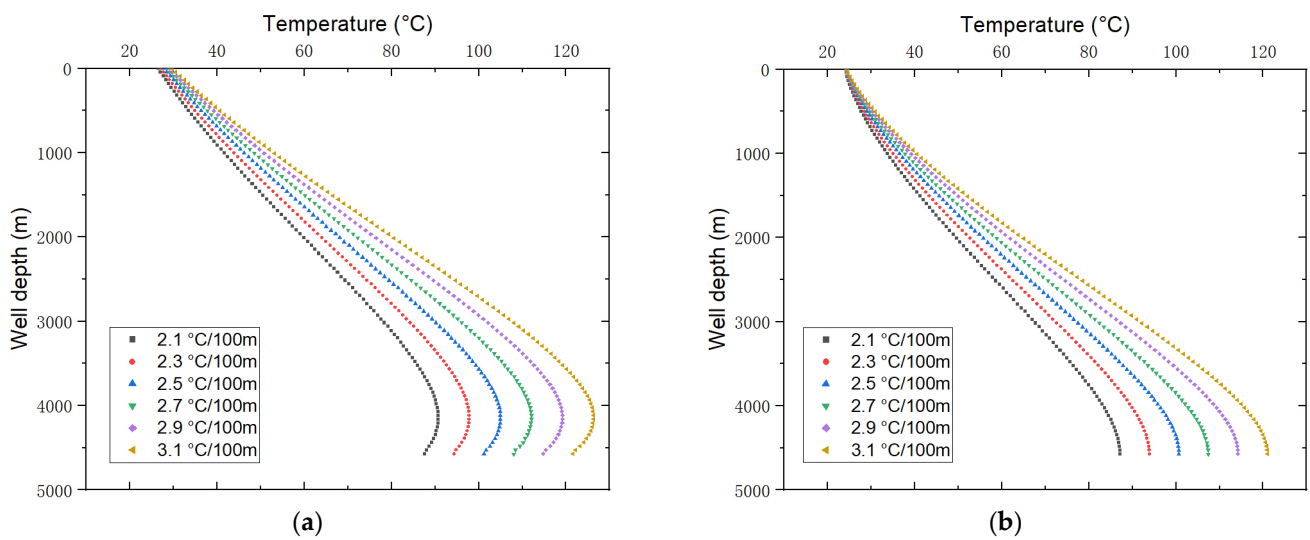

Figure 9. Temperature distribution of drilling fluids with different ground temperature gradients: (**a**) Drilling fluid temperature distribution in the annulus (**b**); Drilling fluid temperature distribution in the casing.

3.3.5. Formation Thermal Conductivity

To clarify the effect of formations with different thermal conductivity on the temperature distribution of drilling fluid, the thermal conductivity is assumed to be 1.5–4.2 W/(m·°C). There are no changes to the other calculation conditions, and the drilling fluid is circulated in the wellbore for 9 h.

From Figure 10a, it can be seen that the effect of thermal conductivity on drilling fluid temperature in the annulus is not significant at the well depth of about 2500 m. As the formation's thermal conductivity increases, the temperature gradually increases below 2500 m and decreases above 2500 m. The thermal conductivity of the formation increases from 1.5 W/(m·°C) to 4.0 W/(m·°C); the hot spot temperature increases by 2.8 °C; and the wellhead temperature decreases by 1.2 °C.
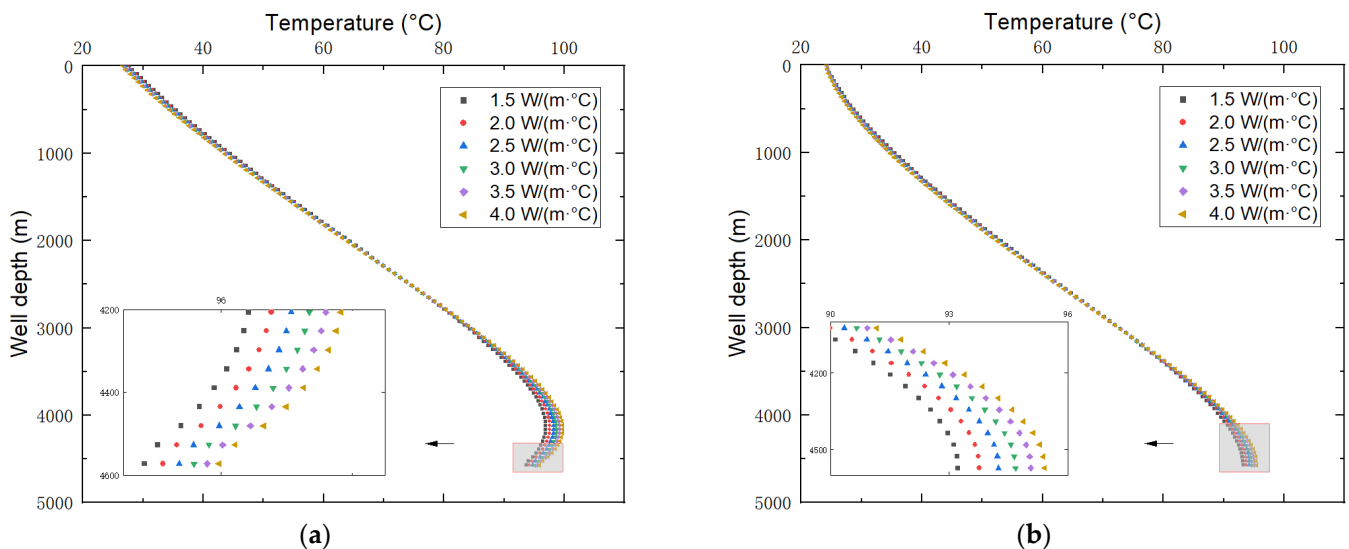
Figure 10. Temperature distribution of drilling fluid for different formation thermal conductivity: (**a**) Drilling fluid temperature distribution in the annulus (**b**); Drilling fluid temperature distribution in the casing.

As shown in Figure 10b, the more the formation thermal conductivity increases, the higher the drilling fluid temperature in the casing. The formation thermal conductivity increased from 1.5 W/(m·°C) to 4.0 W/(m·°C), and the bottom hole temperature increased to 2.2 °C; however, it had less effect on the temperature of wells less than 4000 m deep.

3.3.6. Drilling Fluid Density

Drilling fluid is assumed to be an incompressible fluid with no density change with temperature and pressure, and the effect of density on rheology is also ignored. For drilling fluid densities 1.2–2.2 g/cm^3, variations in temperature distribution (circulation 9 h) are calculated and discussed.

From Figure 11a, it can be seen that in the annulus below 2500 m, the temperature gradually decreases as the density of the drilling fluid increases and the magnitude of the temperature reduction decreases; as the density increases from 1.2 g/cm^3 to 1.4 g/cm^3, the hot spot temperature decreases by 3.3 °C, and as the density increases from 2.0 g/cm^3 to 2.2 g/cm^3, the hot spot temperature decreases by 2.5 °C; as the annulus extends above 2500 m, the temperature gradually increases, the density increases from 1.2 g/cm^3 to 2.2 g/cm^3, and the exit temperature increases by 5.6 °C.

From Figure 11b, it can be seen that with an increase in drilling fluid density, the temperature above 1000 m does not change much, and below 1000 m, the temperature decreases and the decrease gradually diminishes; density increases from 1.2 g/cm^3 to 1.4 g/cm^3; the bottom hole temperature decreases by 3.8 °C; density increases from 2.0 g/cm^3 to 2.2 g/cm^3; and the bottom hole temperature decreases by 2.9 °C.
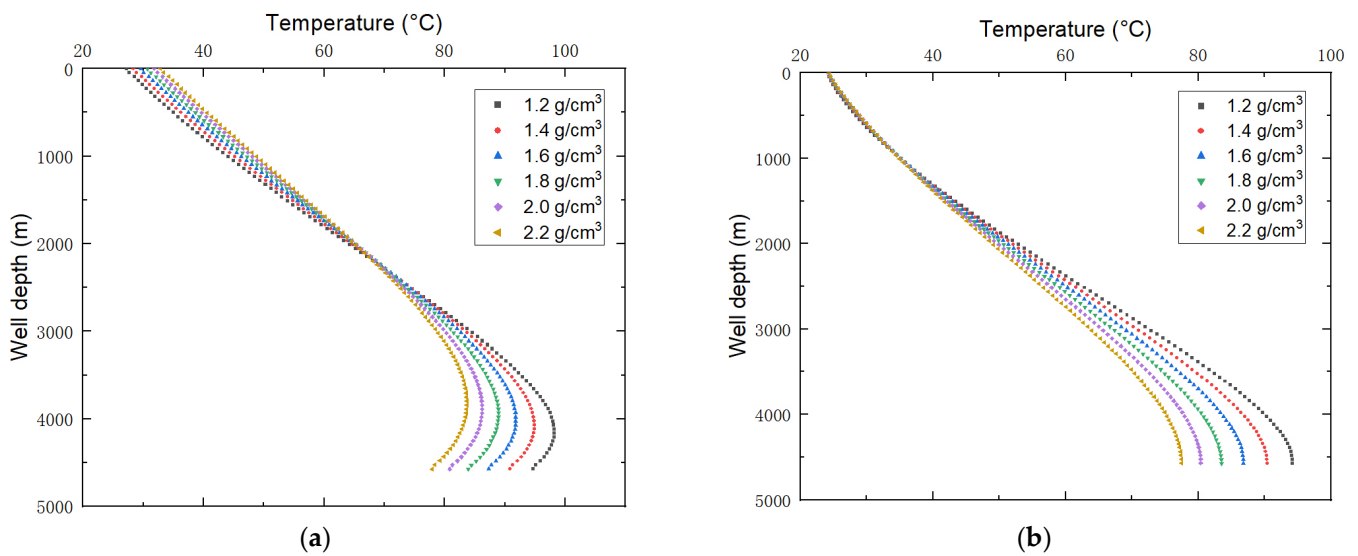
Figure 11. Variations in temperature distribution for different drilling fluid densities: (**a**) Drilling fluid temperature distribution in the annulus (**b**); Drilling fluid temperature distribution in the casing.

As the density of drilling fluid increases, the internal energy of the same volume of drilling fluid increases, and more heat is required to raise the same temperature. The increase in convective heat transfer coefficient by increasing density is limited, and the temperature increase of drilling fluid from the wellhead to the bottom of the well is reduced. In the case of the 1.2 g/cm^3 density drilling fluid, the temperature difference between the inlet and annular hot spots is 74 °C, while in the case of the 2.2 g/cm^3 density drilling fluid, it is only 59.3 °C.

3.3.7. Drilling Fluid Thermal Conductivity

The drilling fluid thermal conductivity is assumed to be 1.2–2.9 W/(m·°C). The effect of thermal conductivity on the temperature distribution (circulation 9 h) is discussed.

From Figure 12a, it can be seen that as the thermal conductivity of the drilling fluid increases, the temperature in the annulus at a well depth of 3000 m does not change significantly, while the temperature below 3000 m gradually increases. The trend is reversed above 3000 m: with the increase in thermal conductivity, the temperature at the bottom of the well gradually increases; the outlet temperature gradually decreases; both temperature changes gradually decrease; the thermal conductivity increases from 1.2 to 1.5 W/(m·°C); the hot spot temperature increases by 0.8 °C; the outlet temperature decreases by 0.29 °C; the thermal conductivity increases from 2.4 to 2.7 W/(m·°C); the hot spot temperature increases by 0.6 °C; and the outlet temperature decreases by 0.18 °C.

From Figure 12b, it can be seen that with an increase in thermal conductivity, the temperature inside the casing gradually rises, but the magnitude of the rise decreases; taking the temperature of the hot spot at the bottom of the well as an example, the thermal conductivity increases from 1.2 to 1.5 W/(m·°C) with a temperature increase of 1.3 °C and from 2.4 to 2.7 W/(m·°C) with a temperature increase of only 0.8 °C.

Thermal conductivity mainly reflects the change in thermal resistance between the fluid and the ground. Thermal conductivity is inversely proportional to thermal resistance. Thermal resistance between the drilling fluid and the formation and casing decreases as thermal conductivity increases.

3.3.8. Drilling Fluid Specific Heat Capacity

In this paper, the specific heat capacity of drilling fluids is assumed to be 1600–4000 J/(kg·°C), and its effect on temperature distribution is considered. Variations in specific heat capacity are generally related to the composition and density of the drilling fluid.
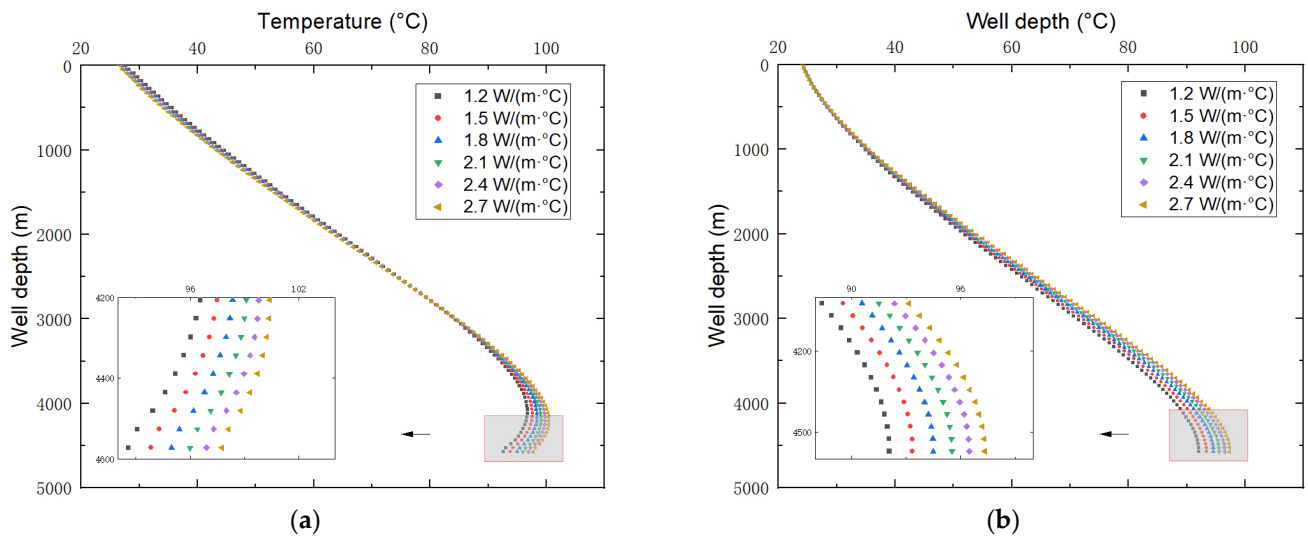
Figure 12. Temperature distribution for different thermal conductivity of drilling fluid: (**a**) Drilling fluid temperature distribution in the annulus (**b**); Drilling fluid temperature distribution in the casing.

Figure 13a illustrates the temperature distribution of drilling fluids with differing specific heat capacities in the annulus. The temperature does not change much as the specific heat capacity of the drilling fluid increases at a well depth of approximately 2100 m, decreases below 2000 m, and increases above 2000 m. Gradually, the magnitude of the temperature change in the whole well decreases. Specific heat capacity increases from 1600 J/(kg·°C) to 4100 J/(kg·°C), hot spot temperatures decreased by 23.9 °C, and outlet temperature increases by 9.3 °C. The temperature change is significant. Specific heat capacity increases from 1600 J/(kg·°C) to 2100 J/(kg·°C), hot spot temperature decreases by 6 °C, and outlet temperature increases by 2.2 °C. Specific heat capacity increases from 3600 J/(kg·°C) to 4100 J/(kg·°C), hot spot temperature decreases by 3.7 °C, and outlet temperature increases by 1.4 °C. Figure 13b shows that as the specific heat capacity of drilling fluid increases, the temperature inside the casing gradually decreases and the decrease diminishes.
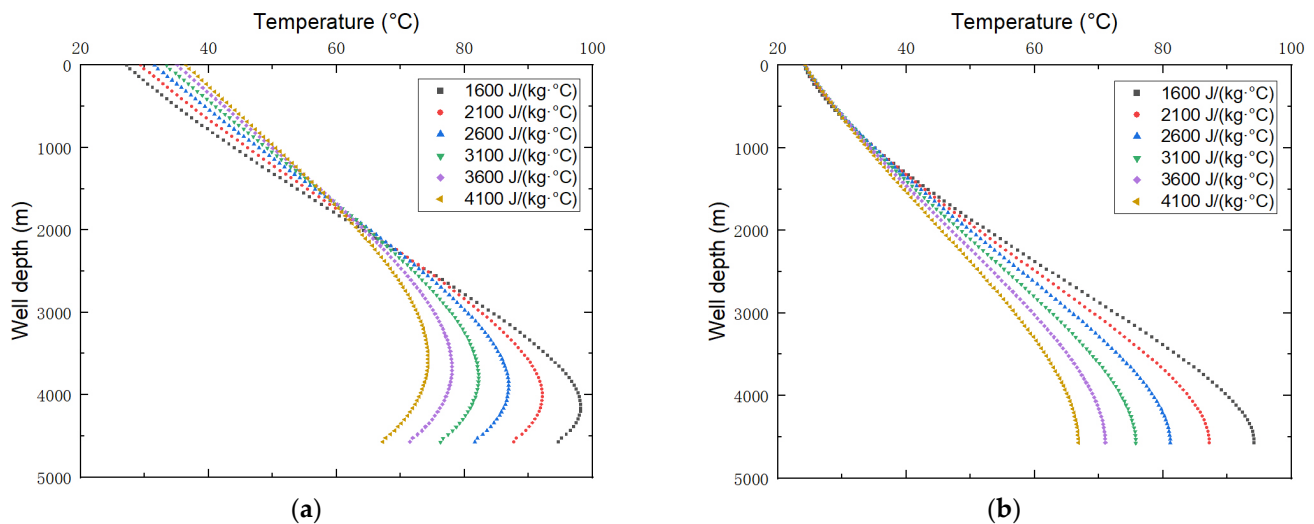

Figure 13. Temperature distribution of drilling fluids with different specific heat capacities: (**a**) Drilling fluid temperature distribution in the annulus (**b**); Drilling fluid temperature distribution in the casing.

Specific heat capacity and density have similar effects on the temperature distribution of drilling fluid. When the specific heat capacity of drilling fluids increases, the internal

energy of a given volume of drilling fluid increases, and more heat is required to raise the same temperature. In the same amount of time, more heat is obtained from the formation, but drilling fluids with a high specific heat capacity have a lower bottom hole temperature and a higher exit temperature than drilling fluids with a low specific heat capacity.

3.3.9. Ranking of the Degree of Influence

In this paper, the magnitude of the effect of eight factors on the hot spot temperature is calculated to represent the degree of their influence on the fluid circulation temperature and temperature field, respectively. The effects of all factors other than the ground temperature gradient and the inlet temperature on the hot spot temperature values are not linear. Limited by the size of radial thermal resistance and heat transfer time, the hot spot temperature increases or decreases with the equal change of independent variables, and the change decreases gradually. For the problem of nonlinear temperature field changes, the average value in the data, i.e., the middle value of the variable, is used to calculate the magnitude of its effect on the temperature value of the fluid hot spot.

By varying the factor by 10%, Figure 14 shows the rate of change of hot spot temperature. Among the factors affecting circulation temperature, ground temperature gradient, circulation flow, drilling fluid specific heat capacity, and drilling fluid density have significant influence; circulation time, drilling fluid thermal conductivity, and formation thermal conductivity have a general influence; and fluid injection temperature has little influence.
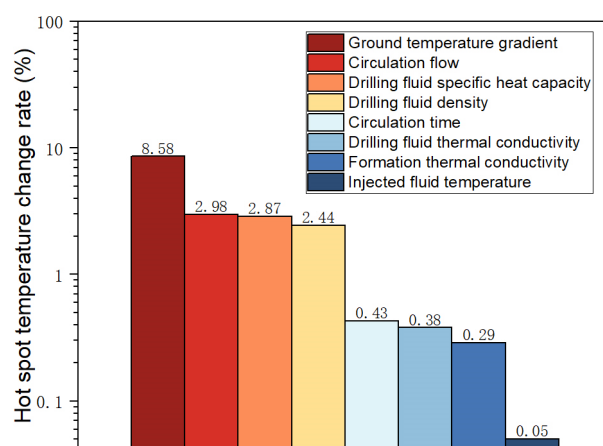

Figure 14. Ranking the degree of influence of 8 factors on hot spot temperature.

The same rules of influence of these factors on drilling fluid circulation temperature apply to cement slurry circulation temperature prediction.

4. Conclusions

The purpose of this paper is to propose an improved method for the prediction of cement slurry circulation temperature in order to increase the safety and lifespan of oil and gas wells, as well as to reduce pollution to the environment. In this method, reasonable initial conditions are obtained in order to improve the accuracy of cement slurry temperature calculations. A circulation wash operation prior to cementing is of the utmost importance in determining the initial conditions. A two-dimensional transient temperature field model is constructed for the temperature field calculation of the cement circulation wash link, and the initial conditions for cement slurry temperature calculation are solved numerically. The influence rules of eight factors on fluid circulation temperature are calculated and discussed, and the degree of their influence on temperature prediction is quantitatively ranked. In conclusion, the following conclusions can be drawn:

(1) If the cementing circulation wash link is taken into account, the initial temperature of the cement slurry temperature calculation will be significantly affected. The temperatures of the wellbore and formation decrease in the lower well section of the well

and increase in the upper well section. As the fluid circulates for 3 weeks, the fluid temperature at the bottom of the well decreases from 120.9 °C to 97.1 °C, and the radial influence distance on formation cooling is 0.75 m. It is foreseen that the cement slurry circulation temperature will be lower and more reasonable under improved initial conditions.

(2) Each factor affects fluid circulation temperature in a different manner and to a different degree. With the increase in circulation time, circulation flow, drilling fluid density, and drilling fluid specific heat capacity, the fluid circulation temperature decreases and the decrease gradually diminishes. As the fluid injection temperature, ground temperature gradient, formation thermal conductivity, and drilling fluid thermal conductivity increase, the circulating temperature of the fluid increases. The temperature increases linearly under the influence of the first two, while the temperature increases gradually slow down under the influence of the last two. Among the factors affecting circulation temperature, ground temperature gradient, circulation flow, drilling fluid specific heat capacity, and drilling fluid density have significant influence; circulation time, drilling fluid thermal conductivity and formation thermal conductivity have a general influence; and fluid injection temperature has little influence.

References

1. Wu, X.; Liu, J.; Li, Z.; Song, W.; Liu, Y.; Shi, Q.; Chen, R. Failure Analysis of Cement Sheath Mechanical Integrity Based on the Statistical Damage Variable. *ACS Omega* **2023**, *8*, 2128–2142. [CrossRef]
2. Bittleston, S.H. A Two-Dimensional Simulator to Predict Circulating Temperatures during Cementing Operations. In Proceedings of the SPE Annual Technical Conference and Exhibition, New Orleans, LA, USA, 23–26 September 1990; OnePetro: Richardson, TX, USA, 1990.
3. Beirute, R.M. A circulating and shut-in well-temperature-profile simulator. *J. Pet. Technol.* **1991**, *43*, 1140–1146. [CrossRef]
4. Honore, R.S., Jr.; Tarr, B.A.; Howard, J.A.; Lang, N.K. Cementing temperature predictions based on both downhole measurements and computer predictions: A case history. In Proceedings of the SPE Production Operations Symposium, Oklahoma City, OK, USA, 21–23 March 1993; p. SPE-25436-MS.
5. Davies, S.N.; Gunningham, M.M.; Bittleston, S.H.; Guillot, F.; Swanson, B.W. Field studies of circulating temperatures under cementing conditions. *Spe Drill Complet.* **1994**, *9*, 12–16. [CrossRef]
6. Guillot, F.; Boisnault, J.M.; Hujeux, J.C. A cementing temperature simulator to improve field practice. In Proceedings of the SPE/IADC Drilling Conference, Amsterdam, The Netherlands, 22–25 February 1993; OnePetro: Richardson, TX, USA, 1993.
7. Aggoun, S.; Cheikh-Zouaoui, M.; Chikh, N.; Duval, R. Effect of some admixtures on the setting time and strength evolution of cement pastes at early ages. *Constr. Build. Mater.* **2008**, *22*, 106–110. [CrossRef]
8. Wojtanowicz, A.K. Environmental Control of Well Integrity. In *Environmental Technology in the Oil Industry*; Springer: Berlin/Heidelberg, Germany, 2016; pp. 61–100.
9. Su, D.; Wu, X.; Li, Z.; Huang, S.; Li, J.; Sun, J.; Zheng, G. Theoretical Analysis of the Micro Annulus of an Oil-Well Cement Sheath Formed via Cooling under Acid-Fracturing Conditions. *Processes* **2022**, *10*, 966. [CrossRef]
10. Liu, J.; Wu, X.; Li, Z.; Song, W.; Liu, Y.; Shi, Q.; Chen, R. Mechanical properties and nonlinear deformation description model of cement stone. *Geoenergy Sci. Eng.* **2023**, *223*, 211578. [CrossRef]
11. Huerta, N.J.; Checkai, D.A.; Bryant, S.L. Utilizing sustained casing pressure analog to provide parameters to study CO_2 leakage rates along a wellbore. In Proceedings of the SPE International Conference on CO_2 Capture, Storage, and Utilization, San Diego, CA, USA, 2–4 November 2009; OnePetro: Richardson, TX, USA, 2009.

12. Zhang, B.; Guan, Z.; Lu, N.; Hasan, A.R.; Xu, S.; Zhang, Z.; Xu, B.; Xu, Y. Control and analysis of sustained casing pressure caused by cement sealed integrity failure. In Proceedings of the Offshore Technology Conference Asia, Kuala Lumpur, Malaysia, 19–23 March 2018; OnePetro: Richardson, TX, USA, 2018.

13. Zhao, C.; Li, J.; Liu, G.; Zhang, X. Analysis of the influence of cement sheath failure on sustained casing pressure in shale gas wells. *J. Nat. Gas. Sci. Eng.* **2019**, *66*, 244–254. [CrossRef]

14. Zhou, Y.; Wojtanowicz, A.K.; Li, X.; Miao, Y. Analysis of gas migration in Sustained-Casing-Pressure annulus by employing improved numerical model. *J. Petrol. Sci. Eng.* **2018**, *169*, 58–68. [CrossRef]

15. Abdelhafiz, M.M.; Hegele Jr, L.A.; Oppelt, J.F. Numerical transient and steady state analytical modeling of the wellbore temperature during drilling fluid circulation. *J. Petrol. Sci. Eng.* **2020**, *186*, 106775. [CrossRef]

16. Wang, R.; Kuru, E.; Yang, X.; Yan, Y.; Yan, X. Prediction of transient wellbore cement circulating temperature distribution using CFD simulation. *J. Petrol. Sci. Eng.* **2021**, *196*, 107912. [CrossRef]

17. Tragesser, A.F.; Crawford, P.B.; Crawford, H.R. A Method for Calculating Circulating Temperatures. *J. Pet. Technol.* **1967**, *19*, 1507–1512. [CrossRef]

18. Sump, G.D.; Williams, B.B. Prediction of wellbore temperatures during mud circulation and cementing operations. *Eng. Ind.* **1973**, *95*, 1083–1092. [CrossRef]

19. Raymond, L.R. Temperature distribution in a circulating drilling fluid. *J. Pet. Technol.* **1969**, *21*, 333–341. [CrossRef]

20. Wang, R.; Wang, Y.; Tyagi, M.; Chen, Y.; Kam, S.I. Multi-dimensional CFD analysis for the prediction of transient wellbore circulating temperature profile to guide offshore cementing job. *J. Korean Soc. Miner. Energy Resour. Eng.* **2019**, *56*, 344–358. [CrossRef]

21. Wong-Loya, J.A.; Andaverde, J.; Santoyo, E. A new practical method for the determination of static formation temperatures in geothermal and petroleum wells using a numerical method based on rational polynomial functions. *J. Geophys. Eng.* **2012**, *9*, 711–728. [CrossRef]

22. Li, Q.; Zhao, D.; Yin, J.; Zhou, X.; Li, Y.; Chi, P.; Han, Y.; Ansari, U.; Cheng, Y. Sediment Instability Caused by Gas Production from Hydrate-bearing Sediment in Northern South China Sea by Horizontal Wellbore: Evolution and Mechanism. *Nat. Resour. Res.* **2023**, 1–26. [CrossRef]

23. Li, Q.; Wang, F.; Wang, Y.; Zhou, C.; Chen, J.; Forson, K.; Miao, R.; Su, Y.; Zhang, J. Effect of reservoir characteristics and chemicals on filtration property of water-based drilling fluid in unconventional reservoir and mechanism disclosure. *Environ. Sci. Pollut. Res.* **2023**, *30*, 55034–55043. [CrossRef] [PubMed]

24. Wang, F.; Shen, K.; Zhang, Z.; Zhang, D.; Wang, Z.; Wang, Z. Numerical simulation of natural gas hydrate development with radial horizontal wells based on thermo-hydro-chemistry coupling. *Energy* **2023**, *272*, 127098. [CrossRef]

25. Edwardson, M.J.; Girner, H.M.; Parkison, H.R.; Williams, C.D.; Matthews, C.S. Calculation of formation temperature disturbances caused by mud circulation. *J. Pet. Technol.* **1962**, *14*, 416–426. [CrossRef]

26. Keller, H.H.; Couch, E.J.; Berry, P.M. Temperature distribution in circulating mud columns. *Soc. Pet. Eng. J.* **1973**, *13*, 23–30. [CrossRef]

27. Marshall, D.W.; Bentsen, R.G. A computer model to determine the temperature distributions in a wellbore. *J. Can. Pet. Technol.* **1982**, *21*, 63–75. [CrossRef]

28. Yang, M.; Li, X.; Deng, J.; Meng, Y.; Li, G. Prediction of wellbore and formation temperatures during circulation and shut-in stages under kick conditions. *Energy* **2015**, *91*, 1018–1029. [CrossRef]

29. Petukhov, B.S. Heat transfer and friction in turbulent pipe flow with variable physical properties. In *Advances in Heat Transfer*; Elsevier: Amsterdam, The Netherlands, 1970; Volume 6, pp. 503–564.

30. Holmes, C.S.; Swift, S.C. Calculation of circulating mud temperatures. *J. Pet. Technol.* **1970**, *22*, 670–674. [CrossRef]

31. Kabir, C.S.; Hasan, A.R.; Kouba, G.E.; Ameen, M.M. Determining circulating fluid temperature in drilling, workover, and well control operations. *SPE Drill Complet.* **1996**, *11*, 74–79. [CrossRef]

32. Ramey, H.J. Wellbore heat transmission. *J. Pet. Technol.* **1962**, *14*, 427–435. [CrossRef]

33. Arnold, F.C. Temperature variation in a circulating wellbore fluid. *J. Energy Resour. Technol.* **1990**, *112*, 79–83. [CrossRef]

34. Wang, R.; Kuru, E.; Yan, Y.; Yang, X.; Yan, X. Sensitivity analysis of factors controlling the cement hot spot temperature and the corresponding well depth using a combined CFD simulation and machine learning approach. *J. Petrol. Sci. Eng.* **2022**, *208*, 109617. [CrossRef]

35. Zhang, Z.; Xiong, Y.; Pu, H.; Sun, Z. Effect of the variations of thermophysical properties of drilling fluids with temperature on wellbore temperature calculation during drilling. *Energy* **2021**, *214*, 119055. [CrossRef]

36. Yang, M.; Luo, D.; Chen, Y.; Li, G.; Tang, D.; Meng, Y. Establishing a practical method to accurately determine and manage wellbore thermal behavior in high-temperature drilling. *Appl. Energy* **2019**, *238*, 1471–1483. [CrossRef]